

Novel function of Roxadustat (FG-4592) as an anti-shock drug in sepsis by regulating mitochondrial oxidative stress and energy metabolism

Guangfeng Long^{a,d,1}, Zhiyin Pei^{a,d,1}, Meng Wu^{a,d,1}, Ke Wei^b, Yang Du^{b,c,d}, Qian Wang^{b,c,d}, Yue Zhang^{b,c,d}, Songming Huang^b, Hongbing Chen^{a,*}, Weiwei Xia^{a,b,c,d,*}, Zhanjun Jia^{b,c,d,*}

^a Department of Clinical Laboratory, Children's Hospital of Nanjing Medical University, Nanjing 210008, China

^b Department of Nephrology, Children's Hospital of Nanjing Medical University, 72 Guangzhou Road, Nanjing 210008, China

^c Jiangsu Key Laboratory of Pediatrics, Nanjing Medical University, Nanjing 210029, China

^d Nanjing Key Laboratory of Pediatrics, Children's Hospital of Nanjing Medical University, Nanjing 210008, China

ARTICLE INFO

Keywords:

Roxadustat
Septic shock
Cardiac dysfunction
Mitochondrial oxidative stress
Energy metabolism

ABSTRACT

Background: Septic shock is a serious clinical syndrome leading to high mortality. A new anti-anemia drug Roxadustat (FG-4592) protected against cardiac injury and hypertension. However, its effect and mechanism on shock and cardiac dysfunction induced by sepsis require to be investigated.

Methods: C57BL/6j mice received FG-4592 (10 mg/kg/day) by i.p injection, followed by lipopolysaccharide (LPS) or cecal ligation and puncture (CLP) treatment. Mortality and shock status were monitored during the experiment. Cardiac function was assessed using echocardiography and serum lactate dehydrogenase (LDH) and creatine kinase-MB (CK-MB) assay. TEM, COX-SDH staining and ATP production were used to evaluate mitochondrial function. A non-targeted metabolomic analysis was performed to evaluate the metabolic disorders.

Results: Both pre- and post-treatment of FG-4592 could improve the survival rate in LPS- and CLP-induced sepsis mice with a better effect in pre-treated animals. Meanwhile, FG-4592 improved systolic blood pressure and body temperature drop in septic mice along with alleviated cardiac dysfunction (as shown by the restoration of decreased LVEF and LVFS and increased LDH and CK-MB) and inflammation. Interestingly, we observed that FG-4592 improved mitochondrial oxidative stress possibly by upregulating the anti-oxidative enzymes of SOD2 and HO-1. Furthermore, FG-4592 improved the energy supply and glycerophospholipid metabolism in cardiomyocytes, possibly through upregulating the HIF-1 α -targeted genes of LDHA and PDK1 in glycolysis and CHK- α , respectively.

Conclusions: FG-4592 protected against mortality and shock in septic animals possibly by antagonizing mitochondrial oxidative stress and metabolic disorders.

General significance: This study provides a potential of FG-4592 as a novel drug for treating septic shock.

1. Introduction

Sepsis is a common systemic inflammatory response syndrome that is mainly caused by endotoxins from gram-negative bacteria during microbial infections. If not treated promptly, severe sepsis/septic shock will lead to uncontrolled release of inflammatory mediators, decreased

tissue perfusion, and subsequent multiple organ failure [1]. Septic shock has a high mortality rate in intensive care units globally. Cardiovascular dysfunction is the leading cause of sepsis-related mortality [2]. Some studies have suggested that sepsis-induced cardiovascular dysfunction and mortality might be attributed to mitochondrial dysfunction [3–5].

During septic shock, glucose concentrations are markedly decreased

Abbreviations: LPS, Lipopolysaccharide; CLP, Cecal ligation and puncture; TEM, Transmission electron microscope; COX-SDH, Cytochrome c oxidase and succinate dehydrogenase; SOD2, Superoxide dismutase 2; HO-1, hemeoxygenase1; HIF-1 α , Hypoxia inducible factor1-alpha; LDHA, Lactate dehydrogenase A; PDK1, Pyruvate dehydrogenase kinase 1; CHK- α , Choline kinase-alpha; eNOS, Endothelial nitric oxide synthase; OCR, Oxygen consumption rate; SBP, Systolic blood pressure; ROS, Reactive oxygen species.

* Corresponding author at: Nanjing Key Laboratory of Pediatrics, Children's Hospital of Nanjing Medical University, Guangzhou Road #72, Nanjing 210008, China.

** Corresponding author at: Department of Clinical Laboratory, Children's Hospital of Nanjing Medical University, Guangzhou Road #72, Nanjing 210008, China.

E-mail addresses: Chenghb1999@126.com (H. Chen), xiawwpku@163.com (W. Xia), jiajz72@hotmail.com (Z. Jia).

¹ These authors contributed equally to this work and share first authorship

<https://doi.org/10.1016/j.bbagen.2022.130264>

Received 28 July 2022; Received in revised form 29 September 2022; Accepted 16 October 2022

Available online 21 October 2022

0304-4165/© 2022 Elsevier B.V. All rights reserved.

in the myocardial muscle, leading to energy deprivation [6]. In addition, myocardial metabolism including a reduction in the oxygen extraction ratio of the myocardium and a lack of choline, changed significantly in septic shock [7–9]. Currently, there is no effective therapy for septic shock except for antibiotics. Therefore, it is necessary to explore new effective treatments for preventing septic shock.

Roxadustat (FG-4592) is a hypoxia-inducible factor (HIF) prolyl hydroxylase inhibitor and got approved on 17 December 2018 as Ai Rui Zhuo® in China for treating anemia in chronic kidney disease (CKD) patients [10]. The drug stabilizes and promotes HIF activity by inhibiting its degradation. As a HIF target gene, endogenous erythropoietin is induced by roxadustat to enhance erythropoiesis. Clinical trials conducted in China showed that oral roxadustat treated CKD patients had higher hemoglobin levels than those in the placebo group [11,12]. To date, >100 HIF target genes that may participate in various physiological and pathological processes have been identified [13], that play roles under hypoxic and non-hypoxic conditions.

According to previous studies, FG-4592 ameliorated cisplatin-induced acute kidney injury (AKI) by inhibiting apoptosis and inflammatory response [14]. FG-4592 retarded AKI-to-CKD transition by improving vascular regeneration and anti-oxidative capability [15]. In cardiovascular diseases, FG-4592 alleviated doxorubicin-induced acute cardiotoxicity through regulating apoptosis and oxidative stress by targeting Bcl-2 and SOD2 [16]. FG-4592 also prevented Ang II-induced hypertension by targeting angiotensin receptors and endothelial nitric oxide synthase (eNOS) [17]. Another group recently reported that FG-4592 protected against sepsis-induced acute lung injury by regulating HIF-1 α and its target gene HO-1 [18]. FG-4592 also increased mitochondrial biogenesis and oxidative respiratory response by regulating the mitochondrial oxygen consumption rate (OCR) and ATP production in SH-SY5Y cells [19]. Moreover, the key enzymes that participate in mitochondrial oxidative energy metabolism are upregulated by FG-4592 treatment [20]. However, the function of FG-4592 during sepsis-induced cardiac dysfunction remains unclear. Therefore, in the present study, we designed experiments to determine the function and potential mechanisms of FG-4592 on cardiovascular dysfunction and survival in septic shock model.

2. Material and methods

2.1. Agents

Lipopolysaccharide (LPS) derived from *Escherichia coli* O111:B4 (no. L2630) was purchased from Sigma-Aldrich (St. Louis, MO, USA). Interleukin-6 (IL-6; no. DKW12-2060-096) and tumor necrosis factor- α (TNF- α ; no. DKW12-2720-096) ELISA kits were purchased from Dakewe Biotech (Shenzhen, China). Roxadustat (FG-4592; no. S1007) was purchased from Selleck Chemicals LLC (Houston, TX, USA). A combined cytochrome C oxidase-succinate dehydrogenase (COX-SDH) staining kit (no. GMS80086.1) was purchased from GENMED (Shanghai, China). Enhanced ATP Assay Kit (no. S0027) was obtained from Beyotime Biotechnology (Shanghai, China). DHE staining kit (BB-470515) was from Bestbio (Nanjing, China). A Dual-Luciferase Assay Kit (no. E1910) was purchased from Promega (Madison, WI, USA).

2.2. Animal models

Male C57BL/6j mice (8–10 weeks old, weighing 22–25 g) were purchased from GemPharmatech Co., Ltd. (Nanjing, China). All mice were housed in a specific pathogen-free (SPF) house with a 12/12 h light/dark cycle and free access to water and food. All procedures were approved by the Nanjing Medical University Institutional Animal Care and Use Committee.

2.3. LPS-induced sepsis model

Male C57BL/6j mice were injected intraperitoneally with LPS (10 mg/kg) to induce septic shock.

2.4. Cecal ligation and puncture (CLP) model

CLP was performed as previously described [21]. Briefly, male C57BL/6j mice were kept anesthetized with 3% isoflurane. A 1.5–2 cm abdominal midline incision was made and the cecum was exposed. The cecum was ligated at 5 mm from the cecum tip and then perforated once with G26 needle. The intestinal contents were manually expelled from the hole to the abdominal cavity. The cecum was softly placed back in the original site and the abdominal incision was closed. In the sham group, the cecum was moved without ligation and puncture.

2.5. Animal experiments protocols

2.5.1. Experiment 1: Effect of FG-4592 on the survival of mice with LPS-induced shock

To evaluate the effect of FG-4592 pre-treatment on the survival of mice with LPS-induced shock, 20 mice were divided into two groups: LPS group ($n = 10$), and FG-4592 + LPS group ($n = 10$). The mice were injected intraperitoneally with vehicle or FG-4592 (10 mg/kg/day) for 48 h before LPS (10 mg/kg) administration. The vehicle or FG-4592 was given daily for 9 consecutive days. Survival was monitored for 7 days. To evaluate the therapeutic effect of FG-4592 on the survival of mice with LPS-induced shock, 20 mice were divided into two groups: LPS group ($n = 10$), and LPS + FG-4592 ($n = 10$) group. The mice were injected with FG-4592 (10 mg/kg/day) in LPS + FG-4592 group 2 h after LPS (10 mg/kg) treatment. The vehicle or FG-4592 was given daily for 7 consecutive days. Survival was recorded for 7 days.

2.5.2. Experiment 2: Effect of FG-4592 on the survival of mice with CLP-induced shock

To evaluate the effect of FG-4592 pre-treatment on the survival of mice with CLP-induced shock, 20 mice were divided randomly into two groups: CLP group ($n = 10$) and FG-4592 + CLP group ($n = 10$). Mice were pretreated with vehicle or FG-4592 (10 mg/kg/day with intraperitoneal) for 48 h before CLP. The vehicle or FG-4592 was given daily for 9 consecutive days. Survival was monitored for 7 days.

To evaluate the therapeutic effect of FG-4592 on the survival of mice with CLP, 20 mice were divided randomly into two groups: CLP group ($n = 10$) and CLP + FG-4592 group ($n = 10$). Mice were injected with FG-4592 (10 mg/kg/day) in the CLP + FG-4592 group 2 h after CLP. The vehicle or FG-4592 was given daily for 7 consecutive days. Survival was recorded for 7 days.

2.5.3. Experiment 3: Effect of FG-4592 on blood pressure and temperature of mice with LPS-induced shock

To demonstrate the effect of FG-4592 on the characteristic indicators of septic shock, mice were divided into two groups: LPS group ($n = 9$) and FG-4592 + LPS group ($n = 8$). FG-4592 + LPS group mice were daily pretreated with FG-4592 (10 mg/kg/day) for 48 h and 2 h before LPS (10 mg/kg) administration. Blood pressure and temperature of mice were measured daily.

2.5.4. Experiment 4: Effect of FG-4592 on cardiac function of mice with LPS-induced shock

To confirm the effect of FG-4592 on the cardiac function of mice with LPS-induced shock, mice were divided into three groups: control group ($n = 10$), LPS group ($n = 10$), and FG-4592 + LPS group ($n = 10$). FG-4592 + LPS group mice were daily pretreated with FG-4592 (10 mg/kg/day) for 48 h and 2 h before LPS (10 mg/kg) administration. Echocardiographic examinations were performed after 12 h of LPS treatment. Blood samples were collected after sacrifice. LDH and CK-MB levels were

measured using an automatic biochemical analyzer.

2.6. Measurement of blood pressure

Systolic blood pressure (SBP) was determined using a non-invasive tail-cuff monitor (BP-2000, Visitech Systems, NC, USA). At least 10 determinations were made in every session, and the mean of the values was taken as the SBP level. All the mice underwent three sessions.

2.7. Echocardiography

Mice were pretreated with FG-4592 (10 mg/kg/day) for 48 h and 2 h before LPS administration. At 12 h after the LPS treatment, mice were anesthetized with isoflurane and echocardiographic examinations were performed using a Vevo 2100 imaging system (VisualSonics, Toronto, ON, Canada).

2.8. Cardiac function and histology

Blood was collected from the inferior vena cava and centrifuged at 3000 rpm for 20 min. Lactate dehydrogenase (LDH), Creatine kinase-MB (CK-MB) levels were measured using an automatic biochemical analyzer. Cardiac tissues were fixed with 4% paraformaldehyde, dehydrated using automatic dehydrator, and embedded in paraffin, 4 μ m thick sections were subjected for hematoxylin and eosin (HE) staining.

2.9. Transmission electron microscopy

Heart tissues were collected and immediately fixed in electron microscope fixed solution. The sections (60 nm) were cut using a microtome. The mitochondrial structure was examined using an electron microscope (JEOL JEM-1010, Tokyo, Japan).

2.10. Combined COX-SDH staining assay

For mitochondrial function studies, fresh mouse heart tissues were embedded with optimal cutting temperature medium (OCT) in liquid nitrogen and 10- μ m-thick sections were collected for combined COX-SDH staining.

2.11. ATP measurement assay

ATP production from heart tissue and cells was measured using an enhanced ATP Assay Kit (no S0027, Beyotime, Shanghai, China) according to the manufacturer's instructions. The protocol was described in a previous study [22].

2.12. Cell culture and treatment

Murine atrial cardiomyocytes (HL-1 cells) and rat heart-derived cardiac cells H9c2 (H9c2 cells) were purchased from the American Type Culture Collection (ATCC). All the two cell lines were cultured in DMEM medium containing 10% FBS (Gibco, Grand Island, NY, USA) in an atmosphere of 5% CO₂ at 37 °C. When the cells reached 70% confluency, they were treated with FG-4592 (2.5, 5, and 10 μ M) for 24 h and then harvested for further analyses.

2.13. Quantitative real-time PCR

Total RNA from mouse heart tissues and cells was extracted using TRIzol reagent (TAKARA, Japan). cDNA was synthesized from 1 μ g of RNAs using reverse transcriptase (2641A, TAKARA, Japan). qRT-PCR was performed using a 7500 PCR system (Applied Biosystems, Foster City, CA) with low ROX SYBR Mix (Vazyme, Nanjing, China). The primers used in this study are listed in Table 1. β -actin was used as the internal reference.

2.14. Immunoblotting

Heart tissues and cultured H9c2 cells were lysed with RIPA buffer containing protease inhibitor cocktail. The cell lysates were centrifuged at 12,000 rpm for 15 min at 4 °C. The BCA method was performed to measure the concentration of the supernatants. Proteins (50 μ g) were loaded and separated by SDS-PAGE gel after denaturation, and the proteins were transferred onto PVDF membrane following 5% non-fat milk blocking for 1 h. Primary antibodies of SOD2 (1:1000, Cat#ab13533, Abcam); HIF-1 α (1:1000, Cat#10006421, Cayman), LDHA (1:1000, Cat#19987-1-AP, Proteintech), PDK1 (1:1000, Cat#10026-1-AP, Proteintech), HO-1 (1:1000, Cat#10701-1-AP Proteintech), CHK α (1:1000, Cat#13520-1-AP Proteintech), and β -actin (1:2000, Cat#60008, Proteintech) were used to incubate with the membrane at 4 °C overnight followed by the incubation with secondary antibody for 2 h. The blots were detected with an enhanced chemiluminescence detection system (Bio-Rad, Hercules, CA, UK) and analyzed using image lab software.

2.15. Enzyme-linked immunosorbent assay (ELISA)

Serum IL-6 and TNF- α levels were measured using ELISA kits according to the manufacturer's instructions.

2.16. Dual luciferase assay

The luciferase reporter plasmid (pGL3-CHK- α promoter) containing the promoter (−2000 to 0) of CHK- α was constructed. The H9c2 cells were transfected with 250 ng of HIF-1 α plasmid/vector and 250 ng pGL3-CHK- α promoter/pGL3 vector using lipofectamine 2000 in 24-well plates for 24 h. Renilla luciferase reporter plasmid pRL-TK (10 ng) was used as an internal control. The transfected cells were harvested for analysis using a Dual-Luciferase Assay Kit according to the manufacturer's protocol.

2.17. Oxygen consumption rate (OCR) assay

The OCR assay was performed using a Seahorse XF-96 Extracellular Flux Analyzer (Seahorse Bioscience, Copenhagen, Denmark). H9c2 (1 \times 10⁴) cells were seeded onto a seahorse cell culture microplate and treated with FG-4592 (5 μ M and 10 μ M) for 24 h. The assay was performed according the manufacturer's instructions. Briefly, the cell medium was replaced with Seahorse assay media after FG-4592 administration, and the cells were cultured in a carbon dioxide-free incubator for 1 h before measurement of the basal OCR. The injection ports were then loaded with mitochondrial inhibitors: oligomycin (1 mM), the uncoupler carbonyl cyanide 4-trifluoromethoxy-phenylhydrazide, FCCP (3 mM for H9c2), and mitochondrial inhibitor: a mixture of rotenone (0.5 mM) and antimycin A (0.5 mM), OCR measurements were performed over time.

2.18. Reactive oxygen species measurement

The level of ROS in the cardiac tissue was measured with dihydroethidium (DHE). 5 μ m thickness fresh frozen heart sections were incubated with DHE (Bestbio, China) for 30 min at 37 °C. Fluorescent images were taken using a Zeiss LSM710 fluorescence microscope. The mean fluorescence intensity was analyzed using ZEISS imaging software ZEN.

The level of ROS in H9c2 was determined by flow cytometry. Briefly, H9c2 cells were pretreated with FG-4592 and then administrated with LPS for 24 h. The cells were then incubated with 10 μ M DCFH-DA for 20 min. The cells were washed three times and collected for analysis using flow cytometry. The mean fluorescence intensity was measured using the CytExpert software.

Table 1
Sequences of primers for qRT-PCR.

Gene name	Forward primer sequence (5'-3')	Reverse primer sequence (5'-3')
Mouse LDHA	TTCAGCGCGGTTCCGTTAC	CCGGCAACATTACACCAC
Mouse PDK1	GCACTCCTTATTGTTCCGGTGG	CGTCGCAGTTTGGATTATGCT
Mouse β -actin	GAGACCTTCAACACCCACAGC	ATGTCACGCACGATTTCCTCC
Mouse IL-1 β	ACTGTGAAATGCCACCTTTTG	TGTTGATGTGCTGCTGTGAG
Mouse IL-6	ACAAAGCCAGAGTCCTTCAGAGAG	TTGGATGGTCTTGGTCCTTAGCCA
Mouse MCP-1	GCTCTCTCTTCTCCACCAC	ACAGCTTCTTTGGGACACCT
Mouse mt-ATP6	CCATAAATCTAAGTATAGCCATTCCAC	AGCTTTTATGTTTGTGTCGGAAG
Mouse mt-ATP8	ACATTCCCACTGGCACC	GGGGTAATGAATGAGGC
Mousemt-ND4L	GCCATCTACCTTCTTCA	TAGGGCTAGTCTACAGC
Mouse mt-COX1	CAGACCGCAACCTAAACACA	TTCTGGGTGCCCAAGAAT
Mouse mt-COX2	GCCGACTAAATCAAGCAACA	CAATGGGCATAAAGCTATGG
Mouse mt-COX3	CGTGAAGGAACCTACCAAGG	ATTCTGTGGAGGTACAGCA
Mouse mt-ND1	ACACTTATTACAACCAAGAACACAT	TCATATTATGGCTATGGGTCAGG
Mouse mt-ND2	CCATCAACTCAATCTCACTTCTATG	GAATCCTGTAGTGGTGGAAGG
Mouse mt-ND3	CCCCAAATAAATCTGTA	CTCATGGTAGTGGAGGT
Mousemt-ND4	GCTTACGCCAAACAGAT	TAGGCAGAAATAGGAGTGAT
Mousemt-ND5	GCCAACAACATATTTCACTTTTC	ACCATCATCCAATTAGTAGAAAGGA
Mouse mt-ND6	GGGAGATTGGTTGATGTA	ATACCCGCAACAAAGAT
Mouse mt-CYTB	GAGGTTGGTTCCGTTTGG	GTTTGAAGGGTGGGTGAC

2.19. Metabolome analysis of cardiac tissue

We harvested heart tissue from mice in experiment 4 for non-target metabolomics analysis. Non-target metabolomic analysis was performed by Biomarker Technologies Corporation (Beijing, China). In detail, a total of 50 mg heart tissue sample was homogenized with acetonitrile containing methanol, centrifuged, dried and re-dissolved in 50% acetonitrile aqueous solution. 1- μ L sample was injected into an acquity UPLC HSS T3 column (1.8 μ m, 2.1*100 mm, Waters, Milford, MA, USA). The mobile phase for positive and negative ion mode consisted of 0.1% formic acid aqueous solution (phase A) and 0.1% formic acid in acetonitrile (phase B). They were mixed and delivered at a flow rate of 0.4 mL/min with a gradient program as follows: 0–0.25 min; 98% A; 0.25–10 min, 98% A; 10–13 min, 2% A; 13–13.1 min, 2% A; 13.1–15 min, 98% A. A high-resolution mass spectrometer (Waters Xevo G2-XS QTOF, Milford, MA, USA) was used to collect primary and secondary mass spectrometry data. The parameters of the ESI ion source are shown as follows: capillary voltage: 2 kV for positive ion mode or –1.5 kV for negative ion mode; cone voltage: 30 V; ion source temperature: 150 °C; dissolvent gas temperature 500 °C; backflush gas flow rate: 50 L/h; dissolvent gas flow rate: 800 L/h. The raw data is processed by Progenesis QI software, orthogonal partial least squares discriminant analysis (OPLS-DA) and metabolic pathway enrichment analysis were carried out by using the pathway analysis tool of metaboanalyst 5.0 (<https://www.metaboanalyst.ca/>).

2.20. Statistical analysis

All data in this study are shown as means \pm SEM. Data were analyzed using one-way or two-way analysis of variance (ANOVA) or unpaired Student's *t*-test using GraphPad Prism software. Kaplan-Meier analysis was used for the survival time analysis. Statistical significance was set at *P* < 0.05. The exact *p* values were presented in the figure legends.

3. Results

3.1. FG-4592 increased the survival rate of septic mice

To evaluate the effect of FG-4592 on survival in septic shock, we established septic shock mouse models by injecting LPS or performing CLP. First, we performed experiments to evaluate the preventive effect of FG-4592 as designed in Fig. 1A. The LPS group mice had a lower survival rate 7 days after LPS administration or CLP. Strikingly, pretreatment with FG-4592 greatly enhanced the survival rate of mice challenged with LPS or CLP (Fig. 1B&C). Moreover, pretreatment with

FG-4592 completely maintained a 100% survival rate of LPS-treated mice (Fig. 1B). We also evaluated the therapeutic effects of FG-4592 as designed in Fig. 1D. The results shown in Fig. 1E&F show that FG-4592 also significantly enhanced the survival rate of mice challenged with LPS or CLP, although the improvement was not as obvious as that in the pretreatment model. These findings indicate that FG-4592 enhances the survival rate of septic mice.

3.2. FG-4592 reversed the reduction of blood pressure and body temperature

The mice displayed reduced systolic blood pressure and body temperature after LPS injection. Systolic blood pressure and body temperature were recorded during the mice experiment process to further define the effect of FG-4592 on septic shock (Fig. 2A). In agreement with findings of a previous study, LPS significantly reduced systolic pressure and body temperature. In LPS-induced shock, FG-4592 strongly attenuated the decrease in systolic pressure and body temperature (Fig. 2B&C). The above results show that treatment with FG-4592 significantly reverses the LPS-induced decrease in systolic pressure and body temperature.

3.3. FG-4592 improved the cardiac function of mice treated with LPS

To explore the effect of FG-4592 on cardiac function in septic shock mice, we measured cardiac function in experimental mice by echocardiography. As shown in Fig. 2D–F, LPS injection significantly decreased LVEF and LVFS. In contrast, FG-4592 significantly prevented this decrease in LVEF and LVFS, indicating that FG-4592 attenuates LPS-induced left ventricular systolic dysfunction. Serum levels of LDH and CK-MB are known biomarkers of myocardial injury. LPS increased LDH and CK-MB levels compared with control mice, and this increase was significantly attenuated by FG-4592 pretreatment (Fig. 2G&H). Cardiac morphology was evaluated by HE staining. In agreement with the improved cardiac function, FG-4592 pretreatment alleviated the morphological changes in cardiomyocytes induced by LPS (Fig. 2I). These data suggest that FG-4592 ameliorates LPS-induced deterioration of cardiac function and morphology.

3.4. FG-4592 pretreatment attenuated cardiac inflammatory responses in mice caused by LPS

The inflammatory response is one of the major causes of myocardial dysfunction during sepsis. In this study, the effect of FG-4592 treatment on LPS-induced cardiac inflammation was analyzed. QRT-PCR showed

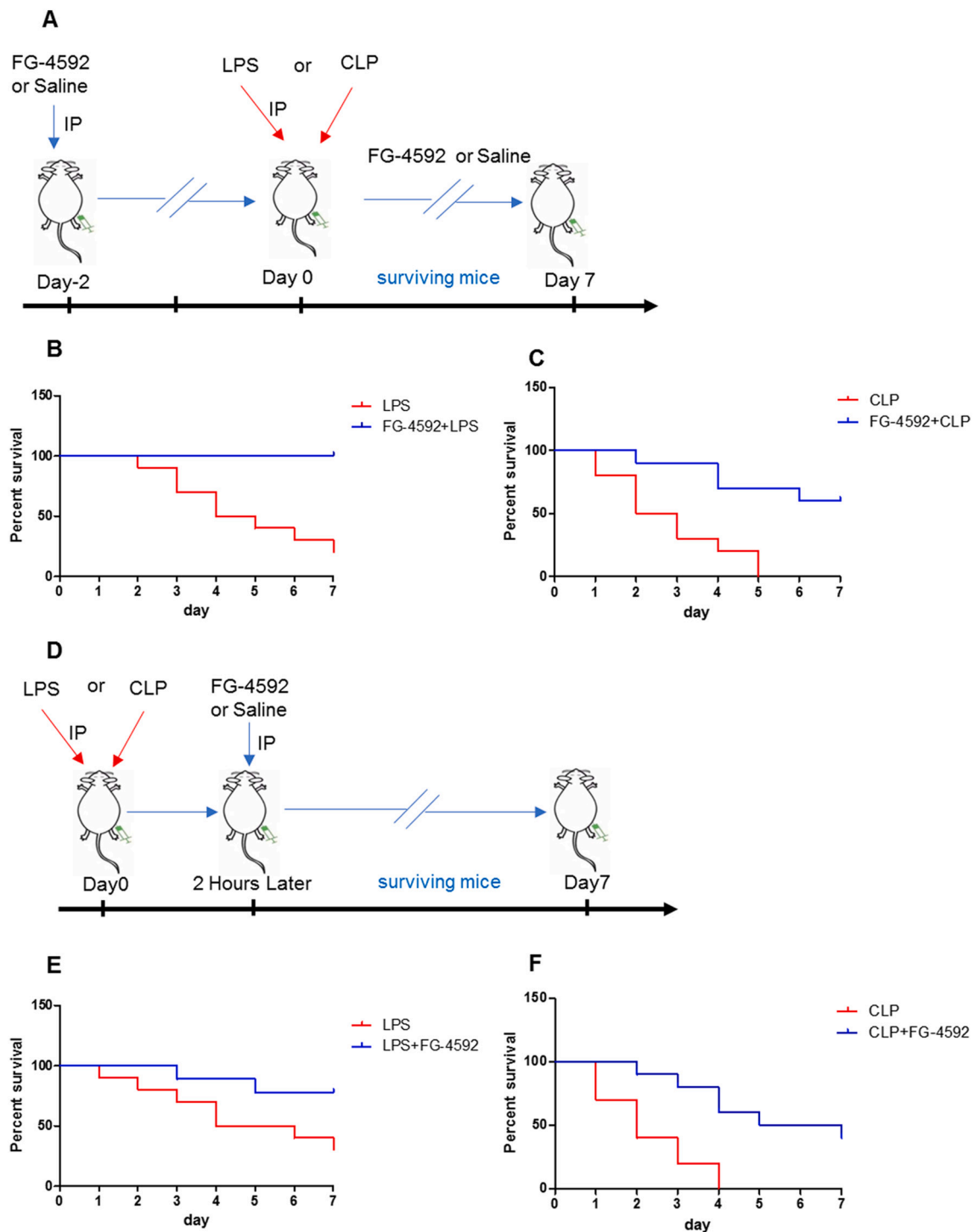


Fig. 1. Effects of FG-4592 on survival rate in septic shock mice.

(A) Animal experimental procedures, mice were injected intraperitoneally with vehicle or FG-4592 (10 mg/kg/day) for 48 h before LPS (10 mg/kg) administration and CLP operation. (B&C) Survival was monitored for 7 days. (D) Animal experimental procedures, mice were injected with FG-4592 (10 mg/kg/day) 2 h after LPS (10 mg/kg) treatment or CLP operation. (E&F) Survival was recorded for 7 days. Colors indicate LPS or CLP group (red), FG-4592 + LPS or FG-4592 + CLP group (blue) ($n = 10$ per group). CLP, cecal ligation and puncture; LPS, lipopolysaccharide.

that the expression of inflammatory factors, including IL-1 β , IL-6, and MCP-1 in the heart, was greatly enhanced by LPS, which was significantly blunted after FG-4592 treatment (Fig. 3A–C). ELISA data showed that the increased circulating protein levels of TNF- α and IL-6 were significantly reduced by FG-4592 (Fig. 3D&E). These data indicate that FG-4592 treatment inhibits the inflammatory response in LPS-induced sepsis. To assess the potential effect of FG-4592 alone on blood

pressure, heart function, morphology and inflammatory factors, we performed an animal experiment with control and FG-4592 groups. The results suggested that FG-4592 had no obvious effect on blood pressure, heart function, morphology and inflammatory factors levels as shown in Fig. S1.

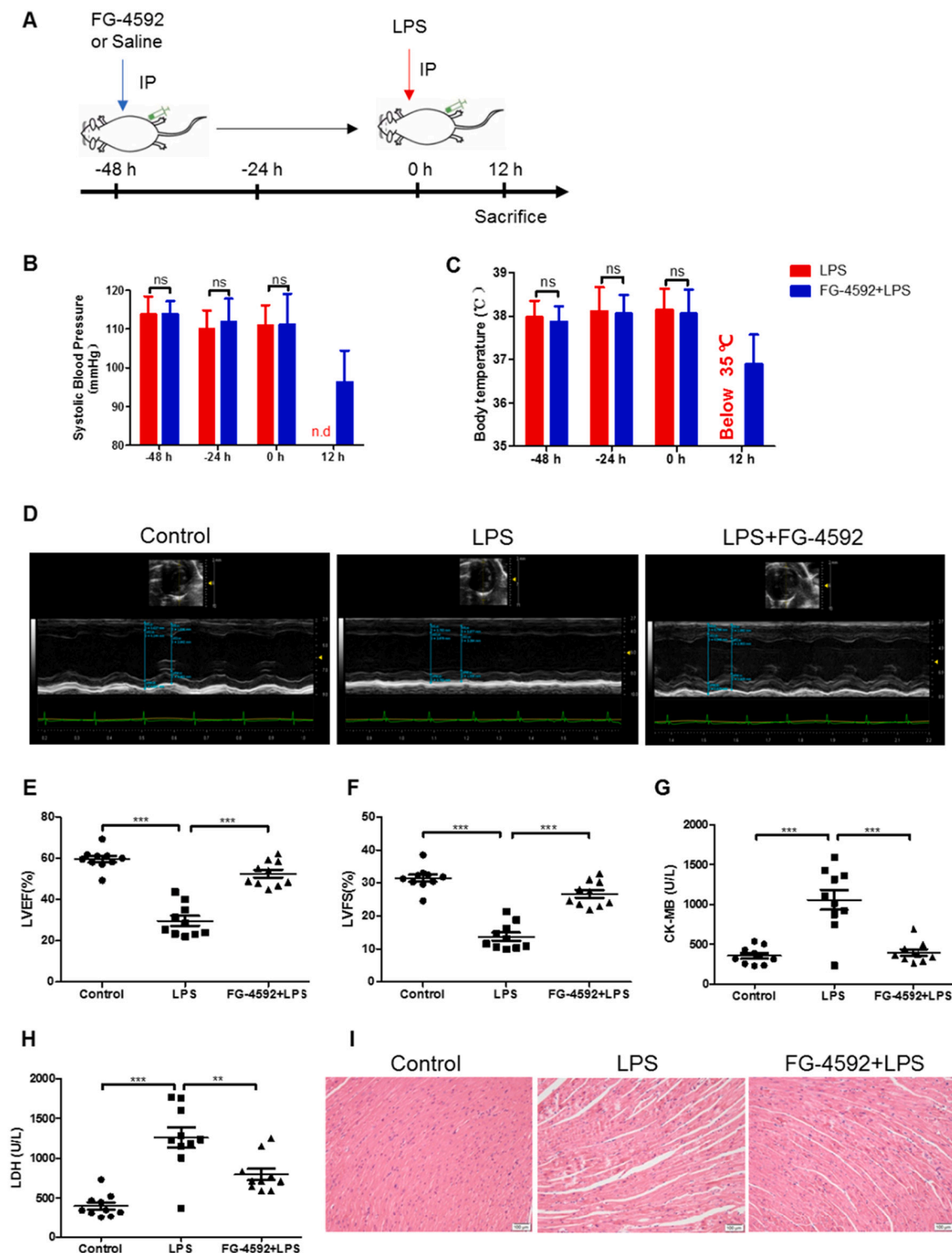


Fig. 2. FG-4592 pretreatment improved blood pressure, body temperature and cardiac function of septic mice.

(A) Mouse treatment scheme. Mice were injected intraperitoneally with vehicle or FG-4592 (10 mg/kg/day) for 48 h before LPS (10 mg/kg) administration. (B&C) systolic pressure (B), body temperature (C) ($n = 8-9$ mice in each group). (D) Cardiac function was examined by echocardiography 12 h after LPS administration. Representative images are shown. (E&F) LVEF and LVFS of experimental animals. (G&H) The levels of circulating CK-MB and LDH ($n = 10$ per group). (I) Representative images of HE staining. The values were represented as mean \pm SEM. One-way ANOVA with Tukey's multiple comparison test analysis and two-way ANOVA with Bonferroni post-tests analysis were used. * $P < 0.05$, ** $P < 0.01$, *** $P < 0.001$. CK-MB, creatine kinase-MB; LDH, lactate dehydrogenase; LPS, lipopolysaccharide; LVEF, left ventricular ejection fraction; LVFS, left ventricular fractional shortening.

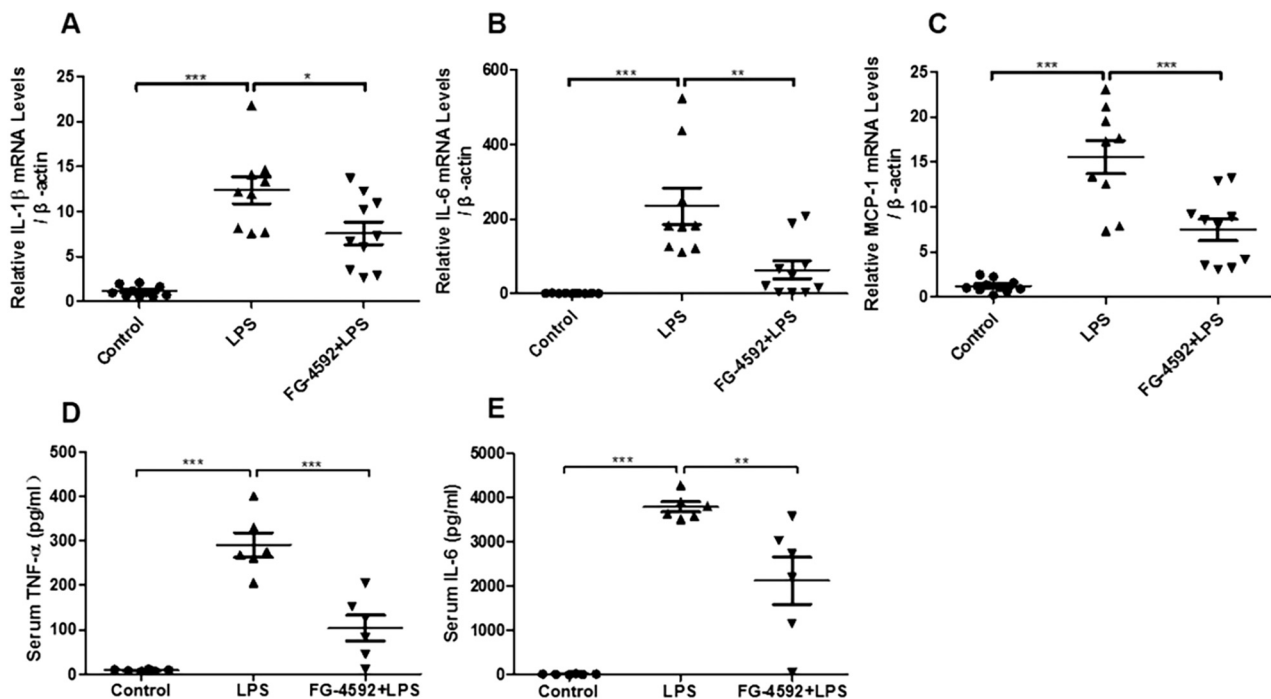


Fig. 3. FG-4592 treatment attenuated cardiac inflammatory responses in septic shock mice.

(A–C) QRT-PCR was performed to detect the mRNA levels of cardiac IL-1 β , IL-6, MCP-1 ($n = 9$ –10 per group). (D&E) The levels of circulating TNF- α (D) and IL-6 (E) was analyzed by ELISA ($n = 6$ per group). The values were represented as mean \pm SEM. One-way ANOVA with Tukey's multiple comparison test analysis was used. * $P < 0.05$, ** $P < 0.01$, *** $P < 0.001$.

3.5. FG-4592 pretreatment attenuated LPS-induced mitochondrial dysfunction in vivo

Mitochondrial dysfunction is another important pathological feature of sepsis-induced heart dysfunction. Therefore, we examined whether FG-4592 treatment could prevent LPS-induced mitochondrial damage. Electron microscopy showed that FG-4592 treatment significantly attenuated the swollen and disrupted cristae of mitochondria in cardiomyocytes of mice treated with LPS (Fig. 4A). COX-SDH staining was performed to analyze the activity of cytochrome C oxidase and succinate dehydrogenase. The results showed that the activity of cytochrome C oxidase and succinate dehydrogenase was markedly decreased by LPS challenge. However, the reduction was partially restored by FG-4592 treatment (Fig. 4B). Furthermore, we examined the mRNA levels of 13 mitochondrial-encoded genes. We found that FG-4592 pretreatment reversed the decrease of most mitochondrial-encoded genes including *ATP6*, *ATP8*, *ND4L*, *COX2*, *ND5* and *ND6*, which are regulated by LPS (Fig. 4C). Moreover, the reduction of ATP in LPS-treated cardiac tissues was significantly restored by FG-4592 (Fig. 4D). These results demonstrate that FG-4592 improves the mitochondrial function.

3.6. FG-4592 alleviated oxidative stress by up-regulating anti-oxidative protein expression

Previous studies have demonstrated that FG-4592 could eliminate ROS levels by upregulating SOD2 and HO-1. In this study, we measured the levels of HIF-1 α , SOD2 and HO-1 in the cardiac tissue. The level of HIF-1 α was decreased in the LPS group and reversed by FG-4592 pretreatment (Fig. 5A&B). The levels of SOD2 and HO-1 were increased in the LPS group and further enhanced by FG-4592 pretreatment (Fig. 5C&D). We also measured the ROS levels of cardiac tissue and found FG-4592 pretreatment significantly decreased the ROS production (Fig. 5E&F). In cultured H9c2 cells, FG-4592 increased the levels of HIF-1 α and its target gene HO-1 in a dose-dependent manner (Fig. 5G–J). Moreover, FG-4592 blocked the LPS-induced increase of ROS levels

(Fig. 5K&L). These findings indicate that FG-4592 inhibits ROS production by enhancing the production of the anti-oxidative stress enzymes SOD2 and HO-1.

3.7. FG-4592 promotes ATP production by enhancing lactate utilization

In sepsis, myocardial metabolism changes significantly, including a reduction in the oxygen extraction ratio and an increase in lactate utilization. In this study, we explored the levels of key enzymes involved in lactate utilization by using QRT-PCR and western blotting. The results indicate that the levels of LDHA and PDK1 were significantly decreased by LPS, which was restored by FG-4592 treatment (Fig. 6A–E). We also examined the intermediate metabolite levels in the Krebs cycle using non-target metabolomics and found that FG-4592 had no effect on citric acid, 1-isopropyl citrate, succinyl-CoA and α -tocopherol succinate levels (Fig. 6F–I). In cultured HL-1 cells, we found that FG-4592 increased the production of ATP and the levels of LDHA and PDK1 (Fig. 7A–D). Consistent with HL-1 cells, FG-4592 increased the production of ATP and the level of LDHA in H9c2 cells (Fig. 7E–H). We further examined the effect of FG-4592 on the oxygen consumption rate (OCR) using seahorse analyzer in H9c2 cells. FG-4592 enhanced OCR and maximal respiratory capacity (Fig. 7I&J). These data demonstrate a potent effect of FG-4592 treatment on ATP production and lactate utilization.

3.8. FG-4592 improved glycerophospholipid metabolism by up-regulating *CHK- α*

We analyzed the data from non-target metabolomics of heart tissues and the OPLS-DA score plots showed a complete separation between control and LPS groups (Fig. 8A) and between LPS and FG-4592 + LPS groups (Fig. 8B). We further analyzed 661 significantly altered metabolites (Fold Change > 2) between Control and LPS groups and 356 altered metabolites (Fold Change > 1.2) between LPS and FG-4592 + LPS groups, and the pathway enrichment analysis showed the metabolites involved in glycerophospholipid metabolism (Phosphatidylcholine,

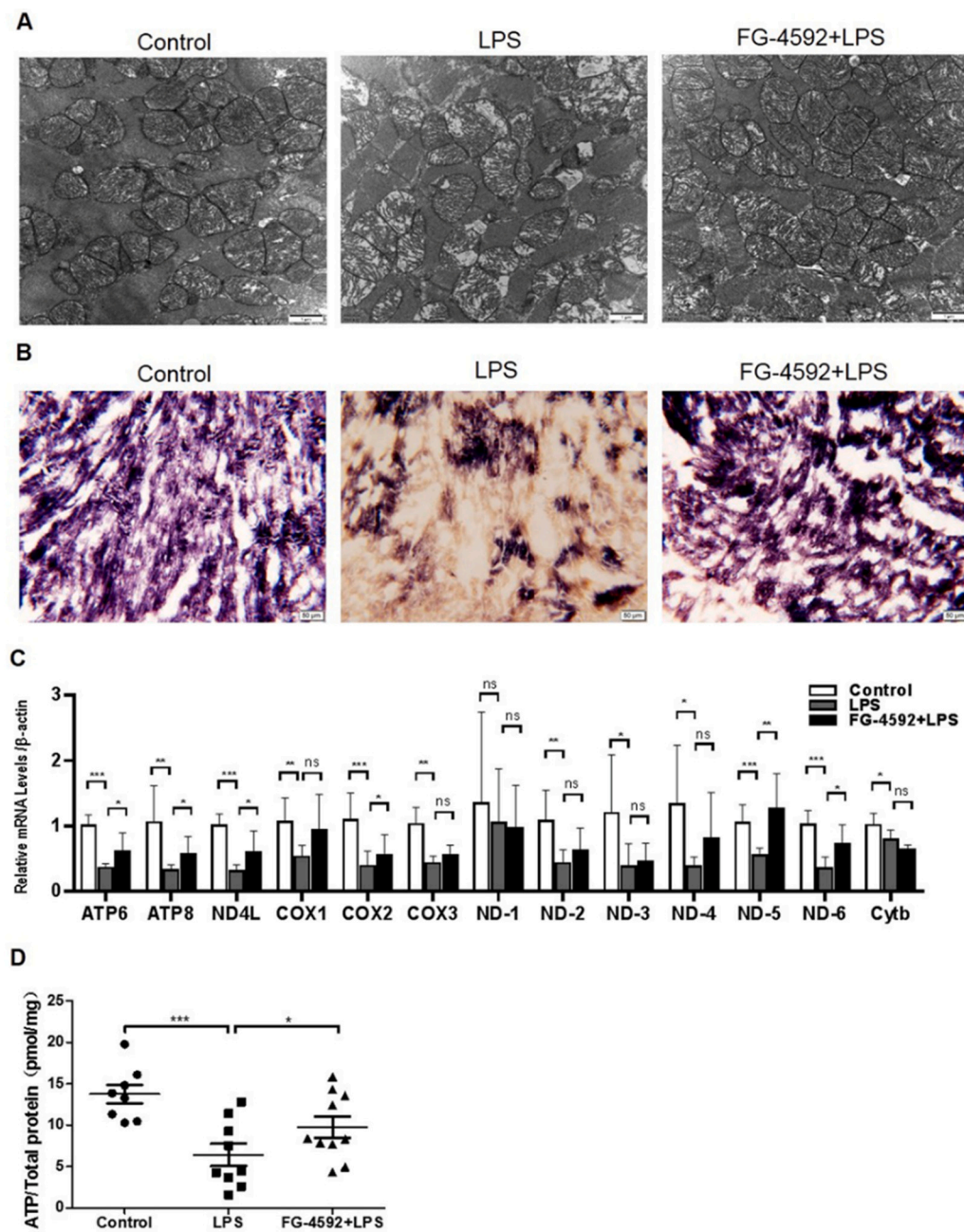


Fig. 4. FG-4592 treatment attenuated LPS-induced mitochondrial dysfunction in vivo.

(A) Representative electron microscopy images of cardiac mitochondria from the left ventricular of experimental animals. (B) Representative COX-SDH staining images from the left ventricular of experimental animals. (C) The mRNA levels of 13 mitochondria-encoded genes in the left ventricular tissues by qRT-PCR ($n = 8$ per group). (D) The ATP production in left ventricular tissue from hearts of mice ($n = 8-10$ per group). The values were represented as mean \pm SEM. One-way ANOVA with Tukey's multiple comparison test analysis was used. * $P < 0.05$, *** $P < 0.001$.

Phosphatidylethanolamine and N-hexadecanoylsphinganine-1-phosphocholine) were significantly up-regulated in the FG-4592 + LPS group (Fig. 8C–G). Also, studies have reported that these metabolites ameliorated organ dysfunction and inflammation caused by endotoxemia [23,24]. Choline kinase- α (CHK- α) is a key enzyme in glycerophospholipid metabolism and a previous study found that HIF-1 α increased CHK- α expression by directly binding to the region of the CHK- α promoter [25]. In cultured H9c2 cells, FG-4592 markedly increased CHK- α expression. Dual luciferase reporter assay results showed that HIF-1 α could activate the CHK- α firefly luciferase reporter (Fig. 8H–J), suggesting that FG-4592 affected glycerophospholipid metabolism possibly by upregulating CHK- α .

Collectively, these results indicate that FG-4592 attenuate sepsis-induced mortality and cardiac dysfunction by improving mitochondrial dysfunction and energy metabolism as shown in Fig. 8K.

4. Discussion

Septic shock is caused by endotoxins and has a high mortality rate. A cascade of events, including the release of many inflammatory mediators, an increase in heart rate, drastic drops in blood pressure and body temperature, decreases in tissue perfusion, and multiple organ failure, occur during the process of septic shock [26]. Some studies indicated that cardiac dysfunction might be the key cause of high mortality in septic patients [27,28]. Accumulating evidence shows that the prevention of heart damage can improve the survival of patients with sepsis [2,29].

Roxadustat (FG-4592) is a new drug for treating anemia in chronic kidney disease patients, and has been reported to play an important protective role in acute kidney diseases [14,30]. Our previous study found that FG-4592 could protect against doxorubicin-induced cardiotoxicity through anti-apoptotic and anti-oxidative pathways [16]. In the present study, we found that FG-4592 could alleviate endotoxic

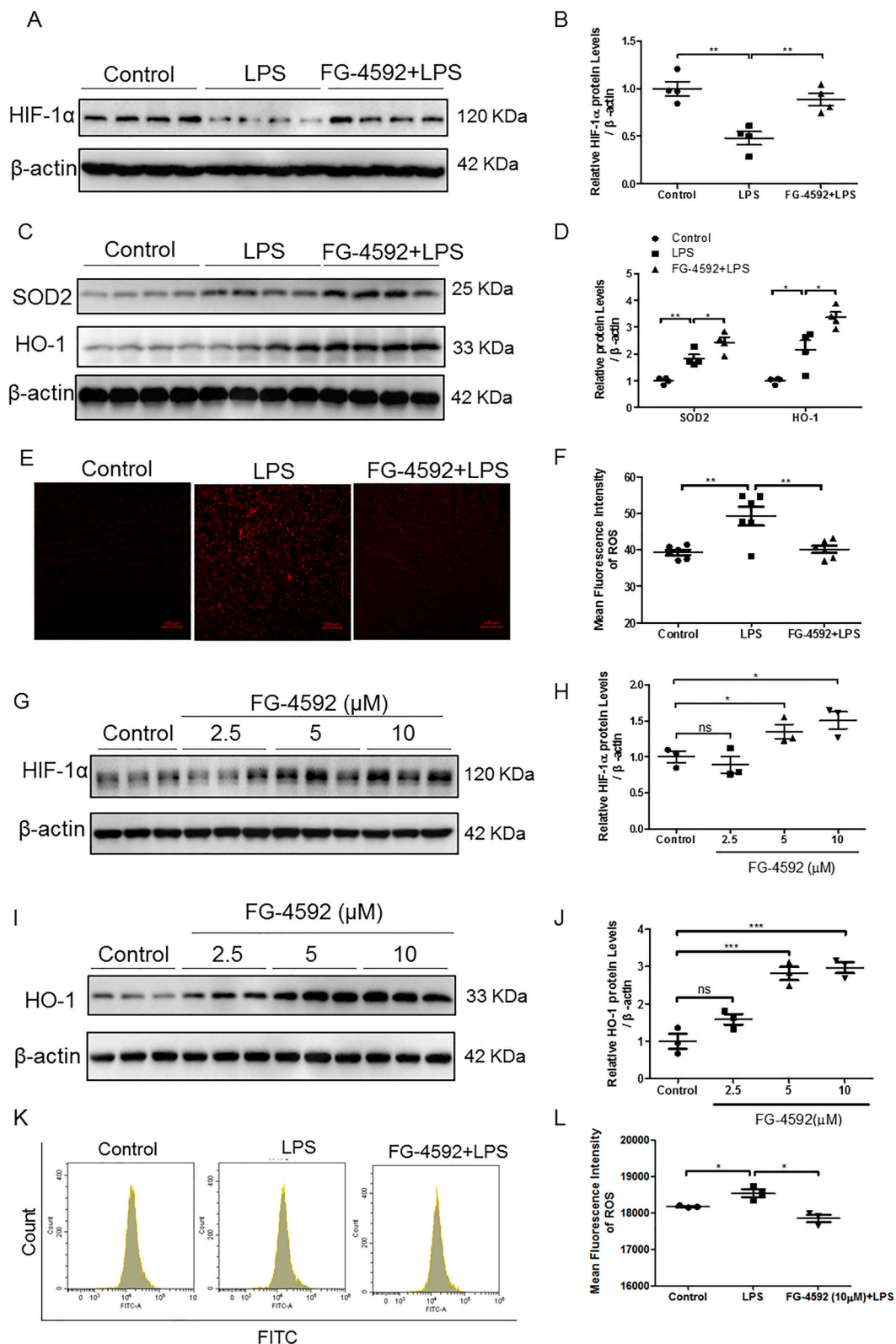


Fig. 5. FG-4592 alleviated oxidative stress by upregulating SOD2 and HO-1.

(A–D) Western blotting was performed to analyze the protein levels of HIF-1α, SOD2 and HO-1 in the heart tissue (*n* = 4 per group). (E&F) Representative images of the DHE staining of cardiac tissue (magnification × 100). Quantitation of the mean fluorescence intensity (*n* = 6 per group). (G&H) Western blotting was performed to analyze the protein level of HIF-1α in H9c2 cells. (I&J) Western blotting was performed to analyze the protein level of HO-1 in H9c2 cells. (K) Representative images of the flow cytometry data from ROS assay in H9c2 cells. The X-axis represents fluorescence intensity, while the Y-axis represents cell counts. (L) Quantitation of the mean fluorescence intensity (MFI). The values are represented as mean ± SEM (*n* = 3 per group). One-way ANOVA with Tukey's multiple comparison test analysis was used. * *P* < 0.05, ***P* < 0.01, ****P* < 0.001.

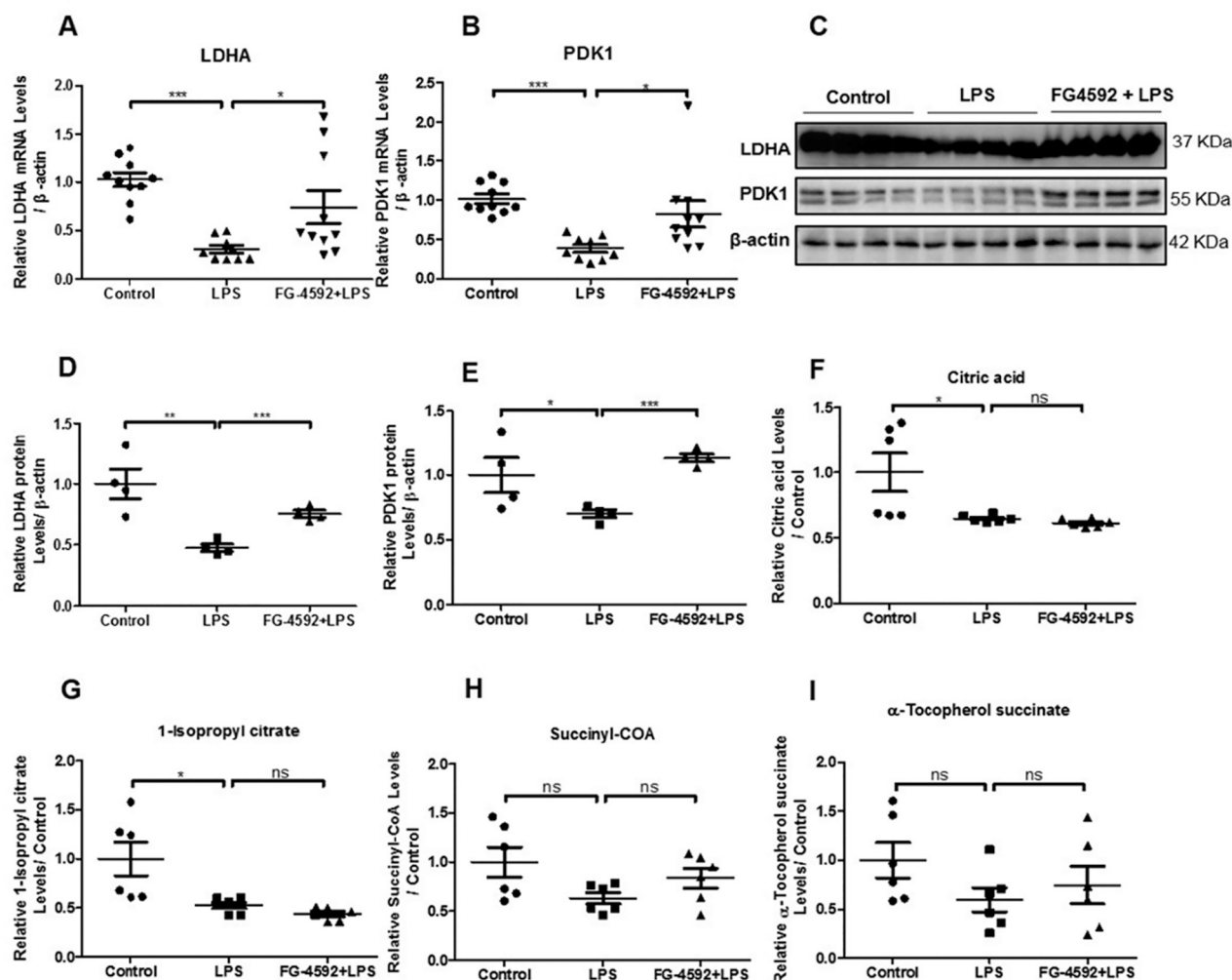


Fig. 6. FG-4592 promoted the expression of key enzymes in lactate utilization.

(A&B) qRT-PCR was performed to analyze the mRNA levels of LDHA and PDK1 in the heart tissue ($n = 9-10$ in each group). (C-E) Western blotting was performed to analyze the protein levels of LDHA and PDK1 in the heart tissue ($n = 4$ in each group). (F-I) The relative levels of citric acid, 1-isopropyl citrate, succinyl-CoA and α -tocopherol succinate from the non-target metabolomics data in the heart ($n = 6$ in each group). The values are represented as mean \pm SEM. One-way ANOVA with Tukey's multiple comparison test analysis was used. * $P < 0.05$, ** $P < 0.01$, *** $P < 0.001$.

shock. First, FG-4592 prolonged the survival time and decreased the mortality of mice induced by LPS or CLP. Moreover, FG-4592 pretreatment completely reversed LPS-induced mortality in mice at a lethal dose, which was more efficiency than post-treatment. Thus, the pre-treatment experimental setting was used for the subsequent and mechanistic investigation. Second, we found that LPS markedly reduced blood pressure and body temperature, which was mostly restored by FG-4592 pretreatment. Third, FG-4592 prevented LPS-induced cardiac dysfunction. Cardiac function after 12 h of LPS treatment was impaired, as shown by the decrease of LVEF, LVFS and the increase of LDH and CK-MB. The experimental results showed that FG-4592 significantly restored the decrease in LVEF, LVFS and the increase in LDH and CK-MB induced by LPS. These findings strongly indicate a protective role of FG-4592 in the improvement of survival rate and cardiac function during septic shock.

Although some studies suggested a protective role of FG-4592 in atherosclerosis [31], cisplatin-induced AKI, folic acid-induced kidney injury [14,30], sepsis-induced acute lung injury [18], and doxorubicin-induced cardiotoxicity [16], perhaps via the regulation of HIF and its target genes that participate in anti-inflammation, anti-apoptosis, anti-oxidative stress, and improving mitochondrial function. However, the role and mechanisms of FG-4592 in survival and cardiac function during

septic shock still require elucidation. It is well known that LPS induces a serious inflammatory response, the major cause of cardiac dysfunction. Previous studies indicated that anti-inflammatory therapies could blunt the inflammatory response and improved the cardiac damage in septic shock. In the present study, the inflammatory factors in circulation (TNF- α and IL-6) and heart (IL-6, IL-1 β and MCP-1) were significantly induced by LPS. Strikingly, FG-4592 pretreatment suppressed the increase in these inflammatory factors, indicating its potent anti-inflammatory effect in septic shock. Some studies have showed that HIF-1 α exacerbates colitis by promoting an inflammatory response [32], while HIF-1 α deletion in macrophages reduced LPS-induced mortality [33]. Our previous work suggested that FG-4592 pretreatment had no effect on the expression levels of TNF- α and IL-6 induced by doxorubicin. Additionally, in agreement with our results, other studies showed that FG-4592 strikingly attenuated inflammation in sepsis-induced acute lung injury and cisplatin induced AKI [14,18]. The multifarious effects of FG-4592 in regulating the inflammatory response might be caused by the activation of different HIF target genes under various conditions or by differences in the pathogenesis of various diseases.

In addition to inflammatory factors, mitochondrial dysfunction and subsequent insufficient energy supply in the heart also contribute to the damage of sepsis-induced cardiac dysfunction and death [34]. Glucose

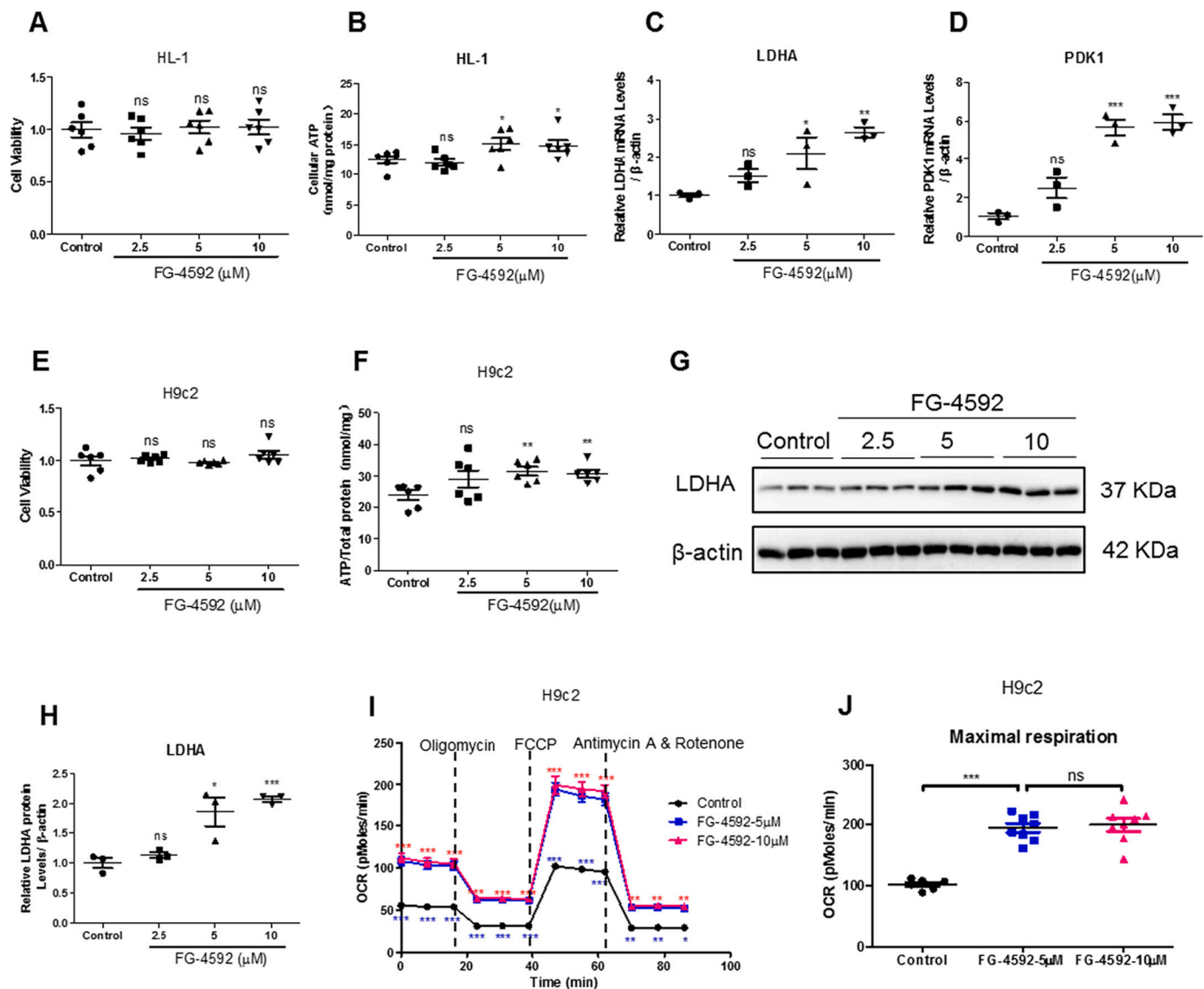
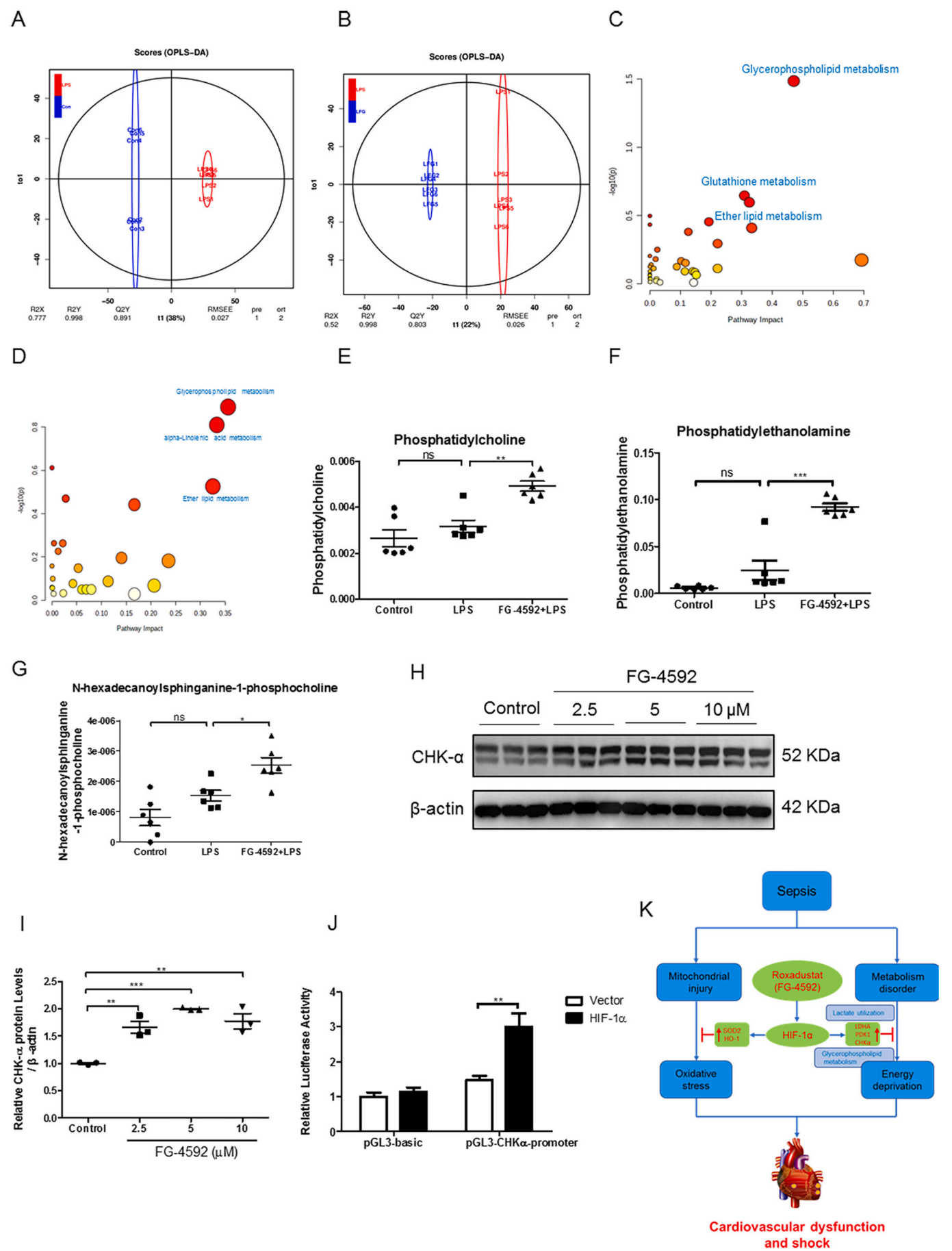


Fig. 7. FG-4592 promotes ATP production and the expression of key enzymes in lactate utilization in HL-1 and H9c2 cells.

(A) Effect of FG-4592 on the cell viability of HL-1 cells after treatment for 24 h ($n = 6$ in each group). (B) Cellular ATP production was detected in HL-1 using a commercial kit ($n = 6$ in each group). (C&D) qRT-PCR was performed to analyze the mRNA levels of LDHA and PDK1 in HL-1 ($n = 3$ in each group). (E) Effect of FG-4592 on the cell viability of H9c2 cells after treatment for 24 h ($n = 6$ in each group). (F) Cellular ATP production was detected in H9c2 ($n = 6$ in each group). (G&H) Western blotting was performed to analyze the protein level of LDHA in H9c2 ($n = 3$ in each group). (I&J) Basal OCR level (Blue stars: control vs FG-4592-5 μM ; red stars: control vs FG-4592-10 μM) (I) and Maximal respiration capacity (J) were detected using a Seahorse XF-96 Extracellular Flux Analyzer ($n = 8$ in each group). The quantitative results are shown as the means \pm SEM. One-way ANOVA with Tukey's multiple comparison test analysis and two-way ANOVA with Bonferroni post-tests analysis were used. * $P < 0.05$, ** $P < 0.01$, *** $P < 0.001$.

oxidation is the main energy source in the heart. LPS reportedly inhibits the expression of key enzymes involved in glucose catabolism and thereby reducing ATP production. Meanwhile, a shift occurred from the use of free fatty acids to utilization of lactate for energy in septic hearts. In this study, we found that LPS induced mitochondrial dysfunction in the heart and the important enzymes (LDHA and PDK1) of glucose oxidation were significantly inhibited in septic hearts. FG-4592 treatment markedly restored the decrease in LDHA and PDK1 in septic hearts. FG-4592 also directly upregulated these key enzymes in cardiomyocytes to increase ATP production. Meanwhile, FG-4592 enhanced its target genes of anti-oxidative enzymes SOD2 and HO-1, which could also protect mitochondria via anti-oxidative action. These results suggest that FG-4592 improves the survival rate and cardiac function during septic shock possibly by regulating mitochondrial oxidative stress, energy supply, and inflammation.

Metabolic alteration also participates in the progression of sepsis-induced cardiac dysfunction. In this study, the non-targeted metabolomic analysis of heart tissues indicated that glycerophospholipid metabolism pathway was significantly changed by FG-4592 pretreatment. In line with our findings, a previous study reported that isosteviol sodium significantly improved cardiac functions under sepsis by altering purine metabolism, glycerophospholipid metabolism, and CoA biosynthesis [23]. Besides, as a key enzyme in glycerophospholipid metabolism, CHK- α expression was regulated by HIF-1 α possibly through direct binding to the region of the CHK- α promoter. We also confirmed that HIF-1 α upregulated the CHK- α expression by binding CHK- α promoter in cardiomyocytes. Therefore, the alteration of glycerophospholipid metabolism could contribute to improved heart function in sepsis by regulating CHK- α .



(caption on next page)

Fig. 8. FG-4592 improved glycerophospholipid metabolism by up-regulating CHK- α .

(A&B) OPLS-DA score plots were generated from non-target metabolomic analysis in heart tissue between Control and LPS group (Blue for control group, red for LPS group) (A), and between LPS and FG-4592 + LPS group (Blue for FG-4592 + LPS group, red for LPS group) (B), and the OPLS-DA score plots showed a significant separation between Control and LPS group, and between LPS and FG-4592 + LPS group. (C) Metabolite pathway enrichment analysis of significantly changed metabolites between Control and LPS group. (D) Metabolite pathway enrichment analysis of significantly changed metabolites between LPS and FG-4592 + LPS group. (E–G) The levels of Phosphatidylcholine, Phosphatidylethanolamine and N-hexadecanoylsphinganine-1-phosphocholine in the heart tissue ($n = 6$ in each group). (H&I) Western blotting was performed to analyze the protein level of CHK- α in H9c2 ($n = 3$ in each group). (J) A dual luciferase reporter assay was performed by transfecting HIF-1 α plasmid/vector and CHK- α promoter firefly luciferase reporter construct ($n = 4$ in each group). (K) Schematic model of proposed protective mechanism of FG-4592 in sepsis-induced cardiovascular dysfunction and shock. The quantitative results were shown as the means \pm SEM. One-way ANOVA with Tukey's multiple comparison test analysis was used. * $P < 0.05$, ** $P < 0.01$, *** $P < 0.001$.

5. Conclusions

In summary, here we reported a potent therapeutic role of FG-4592 in septic shock. The underlying mechanisms of FG-4592 that improve the survival rate and cardiac function could be associated with the activation of HIF-targeted genes SOD2 and HO-1 for regulating mitochondrial oxidative stress and LDHA, PDK1 and CHK- α for glucose oxidation and glycerophospholipid metabolism as shown in Fig. 8K. Our findings extend the clinical use of FG-4592 as an anti-shock drug in sepsis in addition to its application in CKD anemia.

Funding

The work was supported by the National Natural Science Foundation of China [grant numbers 82070760, 82070701, and 82100778]; the Jiangsu provincial maternal and child health research institute [grant numbers JSFY202105, F202155]; the Nanjing National Commission on Health and Family Planning [grant numbers ZKX19042, YKK18146]; and the scientific grants from Nanjing Medical University [grant number NMUB2020038].

Author contributions

Zhanjun Jia, Weiwei Xia, and Hongbing Chen designed the experiments, analyzed data, prepared the figures and wrote the manuscript; Guangfeng Long, Weiwei Xia, Zhiyin Pei, Meng Wu, Ke Wei, Yang Du and Qian Wang performed the experiments; Yue Zhang and Songming Huang contributed to technical advices. All authors reviewed the manuscript.

Data Availability Statement

The data that support the findings of this study are available from the corresponding author upon reasonable request.

CRediT authorship contribution statement

Guangfeng Long: Investigation, Resources, Visualization, Data curation. **Zhiyin Pei:** Investigation, Resources, Visualization, Data curation. **Meng Wu:** Investigation, Resources. **Ke Wei:** Investigation, Visualization. **Yang Du:** Investigation, Visualization. **Qian Wang:** Investigation, Visualization. **Yue Zhang:** Conceptualization, Methodology, Writing – review & editing. **Songming Huang:** Conceptualization, Methodology, Writing – review & editing. **Hongbing Chen:** Conceptualization, Methodology, Writing – review & editing. **Weiwei Xia:** Conceptualization, Investigation, Project administration, Funding acquisition, Writing – original draft, Writing – review & editing. **Zhanjun Jia:** Conceptualization, Supervision, Funding acquisition, Methodology, Writing – original draft, Writing – review & editing.

Declaration of Competing Interest

The authors declare no conflicts of interest.

Data availability

Data will be made available on request.

Appendix A. Supplementary data

Supplementary data to this article can be found online at <https://doi.org/10.1016/j.bbagen.2022.130264>.

References

- [1] M. Cecconi, L. Evans, M. Levy, A. Rhodes, Sepsis and septic shock, *Lancet* 392 (2018) 75–87, [https://doi.org/10.1016/S0140-6736\(18\)30696-2](https://doi.org/10.1016/S0140-6736(18)30696-2).
- [2] M.W. Merx, C. Weber, Sepsis and the heart, *Circulation* 116 (2007) 793–802, <https://doi.org/10.1161/CIRCULATIONAHA.106.678359>.
- [3] J. Larche, S. Lancel, S.M. Hassoun, R. Favory, B. Decoster, P. Marchetti, C. Chopin, R. Neviere, Inhibition of mitochondrial permeability transition prevents sepsis-induced myocardial dysfunction and mortality, *J. Am. Coll. Cardiol.* 48 (2006) 377–385, <https://doi.org/10.1016/j.jacc.2006.02.069>.
- [4] D. Brealey, M. Brand, I. Hargreaves, S. Heales, J. Land, R. Smolenski, N.A. Davies, C.E. Cooper, M. Singer, Association between mitochondrial dysfunction and severity and outcome of septic shock, *Lancet* 360 (2002) 219–223, [https://doi.org/10.1016/S0140-6736\(02\)09459-X](https://doi.org/10.1016/S0140-6736(02)09459-X).
- [5] E.D. Crouser, M.W. Julian, D.V. Blahos, D.R. Pfeiffer, Endotoxin-induced mitochondrial damage correlates with impaired respiratory activity, *Crit. Care Med.* 30 (2002) 276–284, <https://doi.org/10.1097/00003246-200202000-00002>.
- [6] M.S. Chew, K. Shekar, B.A. Brand, C. Norin, A.G. Barnett, Depletion of myocardial glucose is observed during endotoxemic but not hemorrhagic shock in a porcine model, *Crit. Care* 17 (2013) R164, <https://doi.org/10.1186/cc12843>.
- [7] J.F. Dhainaut, M.F. Huyghebaert, J.F. Monsallier, G. Lefevre, J. Dall'Ava-Santucci, F. Brunet, D. Villemant, A. Carli, D. Raichvar, Coronary hemodynamics and myocardial metabolism of lactate, free fatty acids, glucose, and ketones in patients with septic shock, *Circulation* 75 (1987) 533–541, <https://doi.org/10.1161/01.cir.75.3.533>.
- [8] R.E. Cunnion, G.L. Schaer, M.M. Parker, C. Natanson, J.E. Parrillo, The coronary circulation in human septic shock, *Circulation* 73 (1986) 637–644, <https://doi.org/10.1161/01.cir.73.4.637>.
- [9] V. Savci, I.H. Ulus, Cardiovascular effects of central choline during endotoxin shock in the rat, *J. Cardiovasc. Pharmacol.* 30 (1997) 667–675, <https://doi.org/10.1097/00005344-199711000-00018>.
- [10] S. Dhillon, Roxadustat: first global approval, *Drugs* 79 (2019) 563–572, <https://doi.org/10.1007/s40265-019-01077-1>.
- [11] N. Chen, C. Hao, B.C. Liu, H. Lin, C. Wang, C. Xing, X. Liang, G. Jiang, Z. Liu, X. Li, L. Zuo, L. Luo, J. Wang, M.H. Zhao, Z. Liu, G.Y. Cai, L. Hao, R. Leong, C. Wang, C. Liu, T. Neff, L. Szczech, K.P. Yu, Roxadustat treatment for anemia in patients undergoing long-term dialysis, *N. Engl. J. Med.* 381 (2019) 1011–1022, <https://doi.org/10.1056/NEJMoa1901713>.
- [12] N. Chen, C. Hao, X. Peng, H. Lin, A. Yin, L. Hao, Y. Tao, X. Liang, Z. Liu, C. Xing, J. Chen, L. Luo, L. Zuo, Y. Liao, B.C. Liu, R. Leong, C. Wang, C. Liu, T. Neff, L. Szczech, K.P. Yu, Roxadustat for anemia in patients with kidney disease not receiving dialysis, *N. Engl. J. Med.* 381 (2019) 1001–1010, <https://doi.org/10.1056/NEJMoa1813599>.
- [13] J. Schodel, D.R. Mole, P.J. Ratcliffe, Pan-genomic binding of hypoxia-inducible transcription factors, *Biol. Chem.* 394 (2013) 507–517, <https://doi.org/10.1515/hsz-2012-0351>.
- [14] Y. Yang, X. Yu, Y. Zhang, G. Ding, C. Zhu, S. Huang, Z. Jia, A. Zhang, Hypoxia-inducible factor prolyl hydroxylase inhibitor roxadustat (FG-4592) protects against cisplatin-induced acute kidney injury, *Clin. Sci. (Lond.)* 132 (2018) 825–838, <https://doi.org/10.1042/CS20171625>.
- [15] M. Wu, W. Chen, M. Miao, Q. Jin, S. Zhang, M. Bai, J. Fan, Y. Zhang, A. Zhang, Z. Jia, S. Huang, Anti-anemia drug FG4592 retards the AKI-to-CKD transition by improving vascular regeneration and antioxidative capability, *Clin. Sci. (Lond.)* 135 (2021) 1707–1726, <https://doi.org/10.1042/CS20210100>.
- [16] G. Long, H. Chen, M. Wu, Y. Li, L. Gao, S. Huang, Y. Zhang, Z. Jia, W. Xia, Antianemia drug Roxadustat (FG-4592) protects against doxorubicin-induced cardiotoxicity by targeting antiapoptotic and antioxidative pathways, *Front. Pharmacol.* 11 (2020) 1191, <https://doi.org/10.3389/fphar.2020.01191>.

- [17] J. Yu, S. Wang, W. Shi, W. Zhou, Y. Niu, S. Huang, Y. Zhang, A. Zhang, Z. Jia, Roxadustat prevents Ang II hypertension by targeting angiotensin receptors and eNOS, *JCI Insight* 6 (2021), <https://doi.org/10.1172/jci.insight.133690>.
- [18] F. Han, G. Wu, S. Han, Z. Li, Y. Jia, L. Bai, X. Li, K. Wang, F. Yang, J. Zhang, X. Wang, H. Guan, S. Linlin, J. Han, D. Hu, Hypoxia-inducible factor prolyl-hydroxylase inhibitor roxadustat (FG-4592) alleviates sepsis-induced acute lung injury, *Respir. Physiol. Neurobiol.* 281 (2020), 103506, <https://doi.org/10.1016/j.resp.2020.103506>.
- [19] X. Li, X.X. Cui, Y.J. Chen, T.T. Wu, H. Xu, H. Yin, Y.C. Wu, Therapeutic potential of a prolyl hydroxylase inhibitor FG-4592 for Parkinson's diseases in vitro and in vivo: regulation of redox biology and mitochondrial function, *Front. Aging Neurosci.* 10 (2018) 121, <https://doi.org/10.3389/fnagi.2018.00121>.
- [20] I.H. Jain, L. Zazzeron, R. Goli, K. Alexa, S. Schatzman-Bone, H. Dhillon, O. Goldberger, J. Peng, O. Shalem, N.E. Sanjana, F. Zhang, W. Goessling, W. M. Zapol, V.K. Mootha, Hypoxia as a therapy for mitochondrial disease, *Science* 352 (2016) 54–61, <https://doi.org/10.1126/science.aad9642>.
- [21] K.R. Walley, K.R. Thain, J.A. Russell, M.P. Reilly, N.J. Meyer, J.F. Ferguson, J. D. Christie, T.A. Nakada, C.D. Fjell, S.A. Thair, M.S. Cirstea, J.H. Boyd, PCSK9 is a critical regulator of the innate immune response and septic shock outcome, *Sci. Transl. Med.* 6 (2014) 258ra143, <https://doi.org/10.1126/scitranslmed.3008782>.
- [22] Y. Yang, S. Liu, H. Gao, P. Wang, Y. Zhang, A. Zhang, Z. Jia, S. Huang, Ursodeoxycholic acid protects against cisplatin-induced acute kidney injury and mitochondrial dysfunction through acting on ALDH1L2, *Free Radic. Biol. Med.* 152 (2020) 821–837, <https://doi.org/10.1016/j.freeradbiomed.2020.01.182>.
- [23] S. Wang, K.S. Tan, H. Beng, F. Liu, J. Huang, Y. Kuai, R. Zhang, W. Tan, Protective effect of isosteviol sodium against LPS-induced multiple organ injury by regulating of glycerophospholipid metabolism and reducing macrophage-driven inflammation, *Pharmacol. Res.* 172 (2021), 105781, <https://doi.org/10.1016/j.phrs.2021.105781>.
- [24] O. Murch, M. Abdelrahman, M. Collino, M. Gallicchio, E. Benetti, E. Mazzon, R. Fantozzi, S. Cuzzocrea, C. Thiemermann, Sphingosylphosphorylcholine reduces the organ injury/dysfunction and inflammation caused by endotoxemia in the rat, *Crit. Care Med.* 36 (2008) 550–559, <https://doi.org/10.1097/01.CCM.0B013E3181620D2F>.
- [25] K. Glunde, T. Shah, P.T. Winnard Jr., V. Raman, T. Takagi, F. Vesuna, D. Artemov, Z.M. Bhujwalla, Hypoxia regulates choline kinase expression through hypoxia-inducible factor-1 alpha signaling in a human prostate cancer model, *Cancer Res.* 68 (2008) 172–180, <https://doi.org/10.1158/0008-5472.CAN-07-2678>.
- [26] P.E. Spronk, D.F. Zandstra, C. Ince, Bench-to-bedside review: sepsis is a disease of the microcirculation, *Crit. Care* 8 (2004) 462–468, <https://doi.org/10.1186/cc2894>.
- [27] H. Zhou, J. Qian, C. Li, J. Li, X. Zhang, Z. Ding, X. Gao, Z. Han, Y. Cheng, L. Liu, Attenuation of cardiac dysfunction by HSPA12B in endotoxin-induced sepsis in mice through a PI3K-dependent mechanism, *Cardiovasc. Res.* 89 (2011) 109–118, <https://doi.org/10.1093/cvr/cvq268>.
- [28] S. Huang, M. Xu, L. Liu, J. Yang, H. Wang, C. Wan, W. Deng, Q. Tang, Autophagy is involved in the protective effect of p21 on LPS-induced cardiac dysfunction, *Cell Death Dis.* 11 (2020) 554, <https://doi.org/10.1038/s41419-020-02765-7>.
- [29] B. Sun, J. Xiao, X.B. Sun, Y. Wu, Notoginsenoside R1 attenuates cardiac dysfunction in endotoxemic mice: an insight into oestrogen receptor activation and PI3K/Akt signalling, *Br. J. Pharmacol.* 168 (2013) 1758–1770, <https://doi.org/10.1111/bph.12063>.
- [30] X. Li, Y. Zou, J. Xing, Y.Y. Fu, K.Y. Wang, P.Z. Wan, X.Y. Zhai, Pretreatment with Roxadustat (FG-4592) attenuates folic acid-induced kidney injury through antiapoptosis via Akt/GSK-3beta/Nrf2 pathway, *Oxidative Med. Cell. Longev.* 2020 (2020) 6286984, <https://doi.org/10.1155/2020/6286984>.
- [31] X. Zhang, Y. Zhang, P. Wang, S.Y. Zhang, Y. Dong, G. Zeng, Y. Yan, L. Sun, Q. Wu, H. Liu, B. Liu, W. Kong, X. Wang, C. Jiang, Adipocyte hypoxia-inducible factor 2alpha suppresses atherosclerosis by promoting adipose ceramide catabolism, *Cell Metab.* 30 (2019) 937–951, e935, <https://doi.org/10.1016/j.cmet.2019.09.016>.
- [32] Y.M. Shah, S. Ito, K. Morimura, C. Chen, S.H. Yim, V.H. Haase, F.J. Gonzalez, Hypoxia-inducible factor augments experimental colitis through an MIF-dependent inflammatory signaling cascade, *Gastroenterology* 134 (2008) 2036–2048, 2048 e2031–2033, <https://doi.org/10.1053/j.gastro.2008.03.009>.
- [33] C. Peyssonnaud, P. Cejudo-Martin, A. Doedens, A.S. Zinkernagel, R.S. Johnson, V. Nizet, Cutting edge: essential role of hypoxia inducible factor-1alpha in development of lipopolysaccharide-induced sepsis, *J. Immunol.* 178 (2007) 7516–7519, <https://doi.org/10.4049/jimmunol.178.12.7516>.
- [34] Y. Umbarawan, M. Syamsunarno, H. Obinata, A. Yamaguchi, H. Sunaga, H. Matsui, T. Hishiki, T. Matsuura, N. Koitabashi, M. Obokata, H. Hanaoka, A. Haque, F. Kunitomo, Y. Tsushima, M. Suematsu, M. Kurabayashi, T. Iso, Robust suppression of cardiac energy catabolism with marked accumulation of energy substrates during lipopolysaccharide-induced cardiac dysfunction in mice, *Metabolism* 77 (2017) 47–57, <https://doi.org/10.1016/j.metabol.2017.09.003>.